Effect of mechanical strain on magnetic properties of flexible exchange biased FeGa/IrMn heterostructures

Xiaoshan Zhang, Qingfeng Zhan, Guohong Dai, Yiwei Liu, Zhenghu Zuo, Huali Yang, Bin Chen, and Run-Wei Li

Citation: Applied Physics Letters **102**, 022412 (2013); doi: 10.1063/1.4776661
View online: http://dx.doi.org/10.1063/1.4776661
View Table of Contents: http://scitation.aip.org/content/aip/journal/apl/102/2?ver=pdfcov
Published by the AIP Publishing

Effect of mechanical strain on magnetic properties of flexible exchange biased FeGa/IrMn heterostructures

Xiaoshan Zhang, Qingfeng Zhan,[a)] Guohong Dai, Yiwei Liu, Zhenghu Zuo, Huali Yang, Bin Chen, and Run-Wei Li[b)]
Key Laboratory of Magnetic Materials and Devices, Ningbo Institute of Material Technology and Engineering, Chinese Academy of Sciences, Ningbo 315201, People's Republic of China and Zhejiang Province Key Laboratory of Magnetic Materials and Application Technology, Ningbo Institute of Material Technology and Engineering, Chinese Academy of Sciences, Ningbo 315201, People's Republic of China

(Received 4 November 2012; accepted 28 December 2012; published online 16 January 2013)

We have fabricated flexible exchange biased heterostructures with magnetostrictive $Fe_{81}Ga_{19}$ alloy as the ferromagnetic layer and $Ir_{20}Mn_{80}$ as the antiferromagnetic layer on polyethylene terephthalate substrates. The mechanical strain can modify both the strength and the orientation of the uniaxial anisotropy, giving rise to the switching between the easy and hard magnetization directions. Different from the previously reported works on rigid exchange biased systems, a drastic decrease in exchange bias field was observed under a compressive strain with magnetic field parallel to the pinning direction, but only a slightly decrease was shown under a tensile strain. Based on a Stoner-Wohlfarth model calculation, we suggested that the distributions of both ferromagnetic and antiferromagnetic anisotropies be the key to induce the mechanically tunable exchange bias. © *2013 American Institute of Physics*. [http://dx.doi.org/10.1063/1.4776661]

In recent years, giant magnetoresistance (GMR) and tunneling magnetoresistance (TMR) sensors grown on flexible substrates, so called flexible magnetoelectronics, have received widespread attention due to the mechanical deformability and the low processing cost.[1–3] The magnetostriction in magnetic layers coupled with mechanical stress produced by the substrate bending and stretching can often induce a magnetic anisotropy and change the behaviors of flexible spintronic devices.[4] Therefore, for flexible spintronics applied in curved surfaces or used to evaluate the mechanical stress, their magnetic and transport properties under various mechanical stresses need to be known and well controlled. Exchange bias (EB) caused by the interfacial exchange coupling between a ferromagnet (FM) and an antiferromagnet (AFM) is used to stabilize the magnetization of magnetic layers in spin-valve structures and be considered as one of the most crucial factors in determining the performance of flexible spintronic sensors.[5] Technologically, prior to fabricating flexible spin-valve structures with the desirable stress sensitivity, it is necessary to understand how external stress, both compressive and tensile, affects the magnetic characteristics in exchange biased bilayers. The previous works have already studied the effect of stress on magnetic properties for exchange biased systems grown on rigid inorganic substrates, including NiFe/NiO,[6] NiFe/MnIr,[7] and $Fe/Fe_{0.6}Zn_{0.4}F_2(110)$.[8] Using a complex apparatus, the maximum strain in the order of 0.1% can be achieved in stiff substrates, which is far lower than that in flexible films.[7] Han *et al*.[6] found that the coercivity and the uniaxial anisotropy field of NiFe/NiO bilayers deposited on Si wafers are significantly affected by the stress, while the exchange coupling field is apparently not changed by the same stress. Recently, Liu *et al*.[9] reported that in FeMn/NiFe/FeGaB thin films the stress generated by electric field poling the ferroelectric substrates can give rise to a large variation in exchange bias field for magnetic field applied at an angle of 55° with respect to the pinning direction (PD), but almost no change for magnetic field along the PD. So far, the external stress control of magnetic behaviors for flexible exchange biased bilayers is still not well known. In this work, we investigated the effect of mechanical strains on magnetic properties of $Fe_{81}Ga_{19}$/$Ir_{20}Mn_{80}$ bilayers grown on flexible polyethylene terephthalate (PET) substrates. The magnetostrictive $Fe_{81}Ga_{19}$ alloys, which exhibit a large magnetostriction coefficient (~350 ppm for the typical bulk),[10] are selected as the FM layers to improve the response of magnetic properties to the external stress. The magnetic properties including loop squareness, coercivity, and exchange bias field of flexible FeGa/IrMn heterostructures can be effectively tuned by the applied mechanical stresses. Considering the distributions of both FM and AFM anisotropies induced by the residual stress in flexible substrates and the inhomogeneous magnetic field applied during fabrication, a modified Stoner-Wohlfarth model is developed to account for the mechanically tunable EB characteristics.

Exchange biased Ta(5 nm)/$Fe_{81}Ga_{19}$(t_{FeGa})/$Ir_{20}Mn_{80}$ (t_{IrMn})/Ta(30 nm) thin films were deposited on flexible PET plastics using vacuum DC magnetron sputtering with a base pressure below 6×10^{-7} Torr at room temperature. The bottom Ta seeding layers were employed to reduce the roughness of flexible substrates and induce the (111) texture growth of IrMn. The thickness of FeGa layer, t_{FeGa}, is varied from 5 to 25 nm, while the IrMn thickness, t_{IrMn}, is changed from 10 to 100 nm. The samples were protected from oxidation by the Ta capping layers. During deposition, an external magnetic field of 300 Oe provided by a permanent magnet was applied in the plane of films to induce a magnetic easy axis and exchange coupling at the FM/AFM interface. The hysteresis loops for FeGa/IrMn heterostructures under different tensile and compressive strains

a)Electronic mail: zhanqf@nimte.ac.cn.
b)Electronic mail: runweili@nimte.ac.cn.

generated via outward and inward bending the samples were measured by vibrating sample magnetometer (VSM) using a lakeshore model 7400 system at room temperature.

Figure 1(a) shows the typical hysteresis loops for FeGa(10 nm)/IrMn(20 nm) exchange biased bilayers. The EB field, H_{eb}, achieves a maximum value of 69 Oe for magnetic field applied along the induced PD and vanishes for magnetic field perpendicular to the PD. The EB requires the relation $K_{AFM}t_{AFM} \geq J_{ex}$ to be satisfied,[11] where K_{AFM} is the anisotropy of AFM layer, t_{AFM} is the thickness of AFM layer, and J_{ex} is the interface coupling constant. Thus, H_{eb} is significantly influenced by the t_{AFM} dependence of K_{AFM}, when t_{AFM} is comparable to the size of AFM domain wall. For FeGa(10 nm)/IrMn(t_{IrMn}) exchange biased bilayers, H_{eb} significantly increases to 69 Oe by increasing t_{IrMn} to 20 nm, and increases slowly to a constant value by further increasing t_{IrMn}, as displayed in Fig. 1(b). Compared to the exchange biased systems deposited on rigid substrates, H_{eb} reaches saturation usually at the thickness of IrMn below 10 nm.[12] Our x-ray diffraction characterization (not shown) indicates that the (111) texture growth of IrMn on flexible substrate is not as good as on rigid substrates due to the rough surface of flexible substrates, which is probably the reason why the thick AFM layer is needed to saturate H_{eb} in flexible EB systems.

Figure 1(c) shows H_{eb} of FeGa/IrMn bilayers with t_{FeGa} ranging from 5 to 25 nm and t_{IrMn} fixed at 20 and 100 nm. H_{eb} is inversely proportional to t_{FeGa} for a fixed t_{IrMn}, indicating the interfacial effect of EB. The FM/AFM exchange coupling energy can be described as $J_{ex} = H_{eb}M_s t_{FM}$, where M_s is the saturation magnetization of FM film, and t_{FM} is the FM layer thickness. In our experiment, the saturation magnetization of FeGa films is measured about 833 emu/cm^3, which is much less than that of FeGa bulk alloys but comparable with the previously reported values in FeGa films.[13,14] As a result, J_{ex} is obtained to be 0.055 and 0.041 erg/cm^2 for FeGa(t_{FeGa})/IrMn(100 nm) and FeGa(t_{FeGa})/IrMn(20 nm) heterostructures, respectively. J_{ex} is increased with increasing t_{IrMn}. Compared to the exchange coupling energy ($J_{ex} = 0.192$ erg/cm^2) for FeCo/IrMn grown on rigid substrates,[15] J_{ex} of FeGa/IrMn on flexible substrates are much smaller.

As shown in Fig. 1(d), the magnetic field orientation ψ dependence of H_{eb} for FeGa(10 nm)/IrMn(t_{IrMn}) heterostructures with various t_{IrMn} presents a unidirectional symmetry about the PD. To further understanding the phenomenon, we perform numerical calculations based on the Stoner-Wohlfarth model.[16] The total energy of EB system can be given by $E = -K_u \cos^2\theta - K_{eb}\cos\theta - M_S H\cos(\theta - \psi)$, where H is the applied magnetic field, and θ is the angle between magnetization and magnetic easy axis, as indicated in the inset of Fig. 1(d). The unidirectional anisotropy K_{eb} is given by $K_{eb} = H_{eb}M_s$. The induced uniaxial anisotropy K_u is evaluated with the relation $K_u = H_k M_s/2$, where H_k is the magnetic anisotropy field determined from fitting the hysteresis curves measured with magnetic field parallel to the hard axis. For FeGa(10 nm)/IrMn(t_{IrMn}) heterostructures, H_k is obtained to increase from 67 to 200 Oe with increasing t_{IrMn} from 10 to 40 nm, and reach a constant value with further increasing t_{IrMn}. As a result, the uniaxial anisotropy K_u is

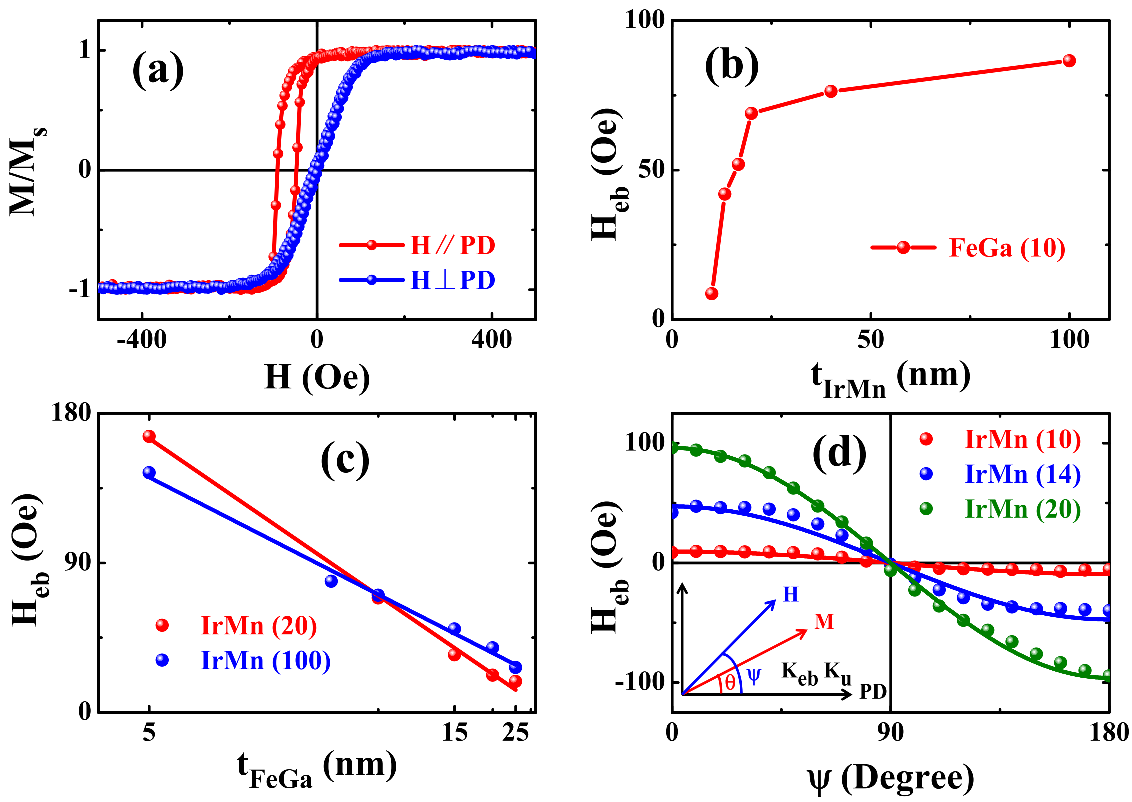

FIG. 1. (a) Typical magnetization curves of the flexible exchange biased FeGa(10 nm)/IrMn(20 nm) heterostructures measured parallel and perpendicular to the PD. (b) t_{IrMn} and (c) t_{FeGa} dependences of H_{eb} for the flexible FeGa/IrMn bilayers. The curves correspond to the $1/t_{\mathrm{FeGa}}$ dependence of H_{eb}. (d) Experimental (symbols) and simulated (continuous lines) H_{eb} as a function of the field orientation ψ for the FeGa(10 nm)/IrMn bilayers with various t_{IrMn}. The geometry of the magnetic anisotropies is shown in the inset of (d).

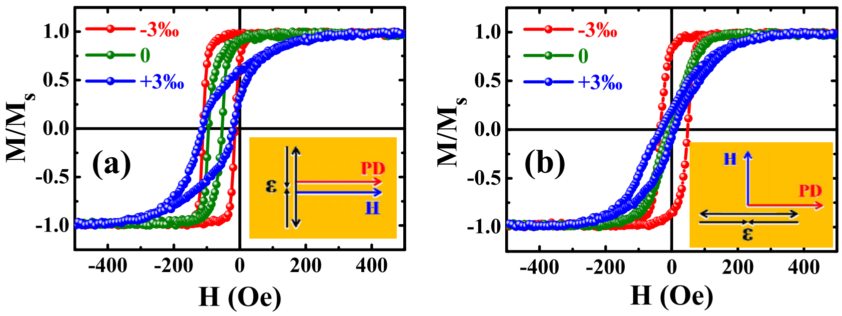

FIG. 2. The applied strain dependence of magnetic hysteresis loops for FeGa(10 nm)/IrMn(20 nm) bilayers with magnetic field (a) parallel and (b) perpendicular to the PD. The compressive and tensile strains are applied perpendicular or parallel to the PD, as shown in the insets of (a) and (b), respectively.

obtained to increase from 2.7×10^4 to 8.3×10^4 erg/cm^3 with increasing t_{IrMn} from 10 to 40 nm. The continuous lines in Fig. 1(d) show the calculated angular dependence of H_{eb}, which agree well with the experimental results.

The effect of mechanical strain on magnetic properties of flexible exchange biased FeGa/IrMn bilayers is systematically investigated. The strain, which is produced by inward or outward bending the flexible samples, is considered to be positive for tensile state, negative for compressive state, and zero for unstrained state. The strain ε can be evaluated using $\varepsilon = T/2\rho$ with T and ρ being the thickness of samples and the curvature radius of bended substrates, respectively. The stress σ is estimated by $\sigma = \varepsilon\ E_f/(1-\nu^2)$, where E_f and ν denote Young's module and Poisson ratio of FeGa film, respectively. Using Young's module $E_f = 60$ GPa for FeGa film and Poisson ratio ν of 0.3 typically for metals,[17] ε is applied within a maximum value of 3‰, which corresponds to $\sigma = 0.2$ GPa. All the samples are mechanically and constantly strained ranging from a compressive strain of -3‰ to a tensile strain of 3‰. Figure 2 shows the typical results for the in-plane strain dependence of normalized magnetic hysteresis loops of FeGa(10 nm)/IrMn(20 nm) bilayers measured by VSM. ε is applied perpendicular or parallel to the PD. In order to restrict H parallel to the surface of films, H is kept perpendicular to ε, i.e., the bending direction, as shown in the insets of Figs. 2(a) and 2(b). When ε is applied perpendicular to the PD, the obvious changes in loop squareness, H_c, and H_{eb} are observed in the strained FeGa/IrMn heterostructures. When H is applied along the PD of FeGa(10 nm)/IrMn(20 nm) films, the increase of tensile strain from 0‰ to 3‰ gives rise to a drastic decrease in the loop squareness from 0.71 to 0.38 and an increase in H_c from 21 to 47 Oe. In contrast, under a compressive strain of -3‰, the loop squareness increases to 0.94 and H_c increases to 48 Oe. H_{eb} decreases significantly from 95 to 86 Oe with increasing the compressive strains from 0‰ to -3‰, and decreases slightly to 93 Oe with increasing the tensile strains to 3‰. As shown in Fig. 2(b), for ε applied parallel to the PD and perpendicular to H, the increase of tensile strain from 0‰ to 3‰ leads to a drastic increase in the squareness from 0.06 to 0.85 and an increase in H_c from 5 to 19 Oe. In contrast, under a compressive strain of -3‰, the squareness slightly increases to 0.17 and H_c increases to 42 Oe. Obviously, in our flexible FeGa/IrMn system, the easy axis of K_u can be swapped with the hard axis under a tensile strain applied perpendicular to the easy axis or a compressive strain parallel to the easy axis. The mechanical strain dependences of loop squareness, H_c, and H_{eb} for flexible FeGa(10 nm)/IrMn(t_{IrMn}) heterostructures with different t_{IrMn} are summarized in Figs. 3(a) to 3(d).

The saturation magnetostriction coefficient λ_s of FeGa film can be estimated using the stress-induced uniaxial anisotropy. For H applied perpendicular to the PD, the EB-induced uniaxial anisotropy $K_u = 1/2H_kM_s$ can be measured. When applying the mechanical stress, the effective anisotropy energy is changed to $E_{eff} = 1/2H_kM_s + 3/2\lambda_s\sigma$. Taking the difference of the two sides of the effective anisotropy energy formula, we obtain $\lambda_s = \Delta H_kM_s/(3\Delta\sigma)$, where the difference of

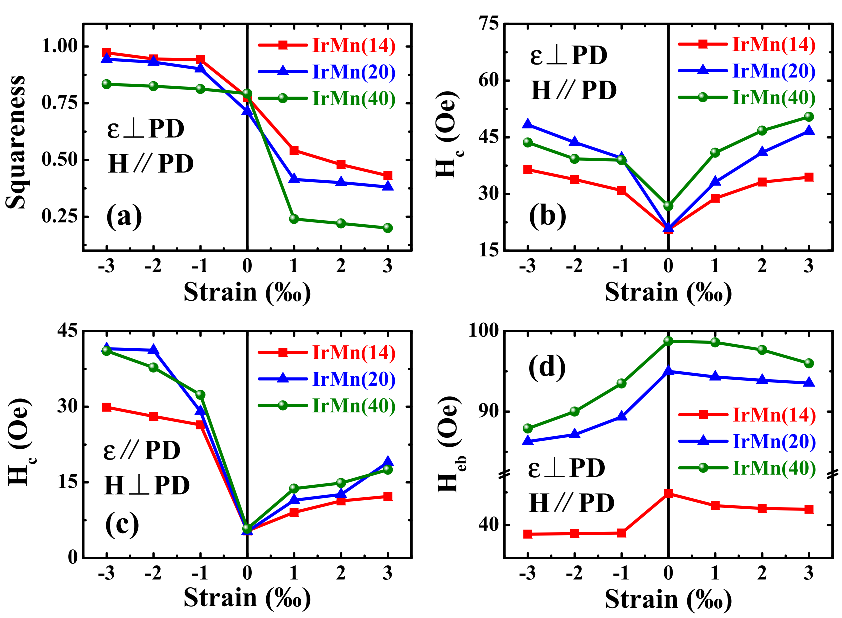

FIG. 3. The applied strain dependence of (a) loop squareness, (b) H_c, and (d) H_{eb} for H parallel and ε perpendicular to the PD, and (d) H_c for H perpendicular and ε parallel to the PD in FeGa(10 nm)/IrMn(t_{IrMn}) bilayers with different t_{IrMn}.

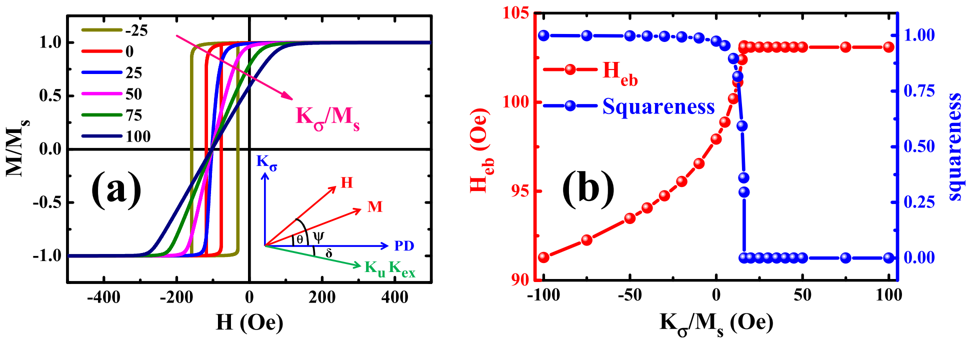

FIG. 4. (a) Calculated hysteresis loops under various stress-induced magnetic anisotropy fields of K_σ/M_s for the flexible exchange biased bilayer with H parallel to the PD using a modified Stoner-Wohlfarth model. The geometries of the magnetic anisotropies and the applied stresses are shown in the inset of (a). (b) The calculated loop squareness (blue line) and H_{eb} (red line) as a function of K_σ/M_s.

the saturation field ΔH_k is experimentally measured as 70 Oe for FeGa(10 nm)/IrMn(20 nm) heterostructures. As a result, we obtained $\lambda_s = 47$ ppm, which is in agreement with the previously reported value for FeGa films.[18] Compared to the high magnetostriction in FeGa single crystals, λ_s has been found to decrease significantly in sputtered FeGa films due to the significant interface contribution to effective magnetostriction.[19]

Theoretically, for an exchange biased system with magnetic field applied along the PD, a compressive stress perpendicular to the PD may enhance the uniaxial anisotropy of films, and therefore align the FM moments along the PD, which cannot lead to any change in the squareness of hysteresis loop and the EB. For a strong tensile stress applied perpendicular to the PD, our simulations based on the Stoner-Wohlfarth model indicate that the squareness can be switched to 0, but the loop shift, i.e., H_{eb} remains unchanged. In our previous work, we consider the distribution of uniaxial anisotropy of the grains in polycrystalline FM layers and qualitatively interpret the mechanically tunable loop squareness in flexible FeGa films.[4] For the present flexible exchange biased system, if only considering the distribution of uniaxial anisotropy in FM layers, that is, a misalignment between FM and AFM spins, H_{eb} predicted using the Stoner-Wohlfarth model remains unchanged regardless the strength of external stresses, which is not consistent with our experimental observations. Due to the inhomogeneous substrate stress and the stray magnetic field during the sample fabrication, the uniaxial anisotropy of AFM layers may be also distributed around the PD of films. Each AFM grain on polycrystalline films interacts with the FM grain on top of it, producing the EB and the unidirectional anisotropy K_{eb}, which is oriented at a small angle of δ with respect to the PD. The EB-induced uniaxial anisotropy K_u of the corresponding FM grain is collinear with K_{eb}. Consequently, for a flexible FeGa/IrMn systems under various external stresses applied perpendicular to the PD, as shown in the inset of Fig. 4(a), the total free energy can be written as $E = -K_u \cos^2(\theta - \delta) + K_\sigma \cos^2\theta - K_{eb} \cos(\theta - \delta) - M_s H \cos(\theta - \psi)$, where K_σ is the external-stress-induced magnetic anisotropy. We assume that the angle of δ for the distribution of both K_u and K_{eb} is ranged from -10 deg to 10 deg with respect to the PD. Based on the magnetization reversal mechanism of coherent rotation, we obtain the hysteresis loops predicted under various K_σ using $K_u/M_s = 20$ Oe, $K_{eb}/M_s = 100$ Oe, and an intermediate value of $\delta = 5$ deg. The simulated magnetization curves of FeGa/IrMn heterostructures gradually become slanted with increasing K_σ/M_s, as shown in Fig. 4(a). The squareness of hysteresis loops increases to 1 with increasing the compressive K_σ/M_s to -50 Oe, and decreases to 0 with increasing the tensile K_σ/M_s to 16 Oe, as shown in Fig. 4(b), which could qualitatively interpret the stress dependence of loop squareness shown in Fig. 3(a). The H_{eb} of flexible FeGa/IrMn heterostructures is significantly affected by the stresses, as shown in Fig. 4(b). The simulated H_{eb} drastically decreases with increasing the compressive stress, and decreases slightly with increasing the tensile stress, which is qualitatively in agreement with the experimental results. Since our model only considers the most dominant factors, a perfect agreement between theory and experiment still cannot be achieved. Obviously, the simulations are able to qualitatively interpret the mechanically tunable EB in flexible FeGa/IrMn heterostructures. In contrast, no substantial change in H_{eb} has been found for the exchange biased bilayer grown on rigid substrates measured in the similar configuration of magnetic field and mechanical stress.[6] Thus, we conclude that the key to induce the tunable EB is the distribution of both FM and AFM anisotropies caused by the residual stress in flexible substrate and the inhomogeneous magnetic field applied during fabrication. It should be noted that the Stoner-Wohlfarth model with considering the distribution of FM and AFM anisotropies can also give almost the same fitting results shown in Fig. 1(d).

In conclusion, we have fabricated a series of exchange biased FeGa/IrMn heterostructures with various thicknesses of FeGa and IrMn layers on flexible PET substrates. By inward and outward bending the samples, the compressive and tensile strain control of uniaxial anisotropy, loop squareness, H_c, and H_{eb} were demonstrated in flexible magnetostrictive FeGa/IrMn heterostructures. In particular, H_{eb} decreases drastically with increasing the compressive stress, and decreases slightly with increasing the tensile stress for magnetic field applied along the PD. Considering the distribution of AFM and FM anisotropies, a modified Stoner-Wohlfarth model was developed to account for the mechanical tunable exchange bias field.

The authors acknowledge the financial support from the National Natural Foundation of China (11174302), State Key Project of Fundamental Research of China (2012CB933004), Zhejiang and Ningbo Natural Science Foundations, and Chinese Academy of Sciences (CAS), and Ningbo Science and Technology Innovation Team (2011B82004).

[1] Y. F. Chen, Y. F. Mei, R. Kaltofen, J. I. Mönch, J. Schuhmann, J. Freudenberger, H.-J. Klauß, and O. G. Schmidt, Adv. Mater. 20, 3224 (2008).
[2] M. Melzer, D. Makarov, A. Calvimontes, D. Karnaushenko, S. Baunack, R. Kaltofen, Y. F. Mei, and O. G. Schmidt, Nano Lett. 11, 2522 (2011).
[3] C. Barraud, C. Deranlot, P. Seneor, R. Mattana, B. Dlubak, S. Fusil, K. Bouzehouane, D. Deneuve, F. Petroff, and A. Fert, Appl. Phys. Lett. 96, 072502 (2010).

[4]G. H. Dai, Q. F. Zhan, Y. W. Liu, H. L. Yang, X. S. Zhang, B. Chen, and R. W. Li, Appl. Phys. Lett. **100**, 122407 (2012).
[5]S. S. P. Parkin, Appl. Phys. Lett. **69**, 3092 (1996).
[6]D.-H. Han, J.-G. Zhu, J. H. Judy, and J. M. Silversten, Appl. Phys. Lett. **70**, 664 (1997).
[7]M. Sonehara, T. Shinohara, T. Sato, K. Yamasawa, and Y. Miura, J. Appl. Phys. **107**, 09E718 (2010).
[8]Ch. Binek, P. Borisov, X. Chen, A. Hochstrat, S. Sahoo, and W. Kleemann, Eur. Phys. J. B **45**, 197 (2005).
[9]M. Liu, J. Lou, S. D. Li, and N. X. Sun, Adv. Funct. Mater. **21**, 2593 (2011).
[10]A. E. Clark, J. B. Restorff, M. Wun-Fogle, T. A. Lograsso, and D. L. Schlagel, IEEE Trans. Magn. **36**, 3238 (2000).
[11]W. H. Meiklejohn, J. Appl. Phys. **33**, 1328 (1962).
[12]J. Nogués and I. K. Schuller, J. Magn. Magn. Mater. **192**, 203 (1999).
[13]J. Atulasimha and A. B. Flatau, Smart Mater. Struct. **20**, 043001 (2011).
[14]B. W. Wang, S. Y. Li, Y. Zhou, W. M. Huang, and S. Y. Cao, J. Magn. Magn. Mater. **320**, 769 (2008).
[15]H. N. Fuke, K. Saito, Y. Kamiguchi, H. Iwasaki, and M. Sahashi, J. Appl. Phys. **81**, 4004 (1997).
[16]E. C. Stoner and E. P. Wohlfarth, Philos. Trans. R. Soc., Ser. A **240**, 599 (1948).
[17]R. A. Kellogg, A. B. Flatau, A. E. Clark, M. Wun-Fogle, and T. A. Lograsso, J. Appl. Phys. **91**, 7821 (2002).
[18]T. Brintlinger, S. H. Lim, K. H. Baloch, P. Alexander, Y. Qi, J. Barry, J. Melngailis, L. Salamanca-Riba, I. Takeuchi, and J. Cumings, Nano Lett. **10**, 1219 (2010).
[19]H. Szymczak, IEEE Trans. Magn. **30**, 702 (1994).